American Mineralogist, Volume 82, pages 280–290, 1997

Al, Si, and Mg occupancies in tetrahedrally and octahedrally coordinated sites in synthetic aluminous tremolite

David M. Jenkins,[1] Barbara L. Sherriff,[2] Janice Cramer,[2] and Zhi Xu[2,*]

[1]Department of Geological Sciences and Environmental Studies, Binghamton University, Binghamton, New York, 13902-6000, U.S.A.

[2]Department of Geological Sciences, University of Manitoba, Winnipeg, Manitoba, R3T 2N2, Canada

Abstract

A series of aluminous tremolites was synthesized at 800–850 °C and 6–13 kbar along the join $Ca_{1.8}Mg_{5.2}Si_8O_{22}(OH)_2$-$Ca_{1.8}(Mg_{4.2}Al)(AlSi_7)O_{22}(OH)_2$ by means of the Mg-Tschermaks substitution. Although the amphibole yields were high (97–99 wt%), traces of orthopyroxene, clinopyroxene, amorphous silica, and, for the most aluminous mixture, corundum, were identified in some synthesis products. The samples were characterized by electron microprobe (EMP), X-ray diffraction Rietveld structure refinement (XRD), Fourier-transform infrared (FTIR) spectroscopy, and magic-angle-spinning nuclear magnetic resonance (MAS NMR) spectroscopy for the purpose of identifying the extent of Al, Mg, and Si order-disorder in the octahedral and tetrahedral sites. Both EMP and ^{27}Al NMR verify that the Mg-Tschermaks substitution, with even distribution of Al between tetrahedral and octahedral sites, is obeyed in these amphiboles up to a limit of 1.9 total Al atoms per formula unit (apfu).

^{29}Si MAS NMR spectra indicate that Al substitutes essentially equally into both the T1 and T2 sites. For octahedral sites, the FTIR spectra indicate the presence of Al on the M1, M3, or both sites (presently indistinguishable) by the presence of an (MgMgAl)-OH band at 3652 cm^{-1}, which increases steadily with increasing Al content. The FTIR and ^{27}Al MAS NMR spectra show that Al is always present in the M1-M3 sites as well as the M2 site but partitioned among these sites in ways that are not clearly resolved at present. It is clear in this study that Al is more widely distributed over the octahedral and tetrahedral sites in synthetic aluminous tremolite with only a moderate Al content ($<$2.0 Al apfu) than has been traditionally thought.

Introduction

Incorporation of Al into calcic amphibole by means of the Tschermaks substitution $^{[4]}Si^{4+} + {}^{[6]}Mg^{2+} = {}^{[4]}Al^{3+} + {}^{[6]}Al^{3+}$ (site coordination in brackets) was first suggested by Warren (1930) and continues to be recognized as an important substitution (Stephenson 1993). Recent experimental work dealing explicitly with the Tschermaks substitution into tremolitic amphiboles along the join $(Ca_{1.8}Mg_{0.2})Mg_5Si_8O_{22}(OH)_2$-$(Ca_{1.8}Mg_{0.2})(Mg_4Al)(AlSi_7)O_{22}(OH)_2$ (Smelik et al. 1994; Jenkins 1994) has focused mostly on the macroscopic effects of this substitution without having the accompanying information on the microscopic aspects of cation-site occupancies. The latter information is of considerable importance in (1) defining or verifying proposed mixing-on-sites activity-composition relationships for calcic amphiboles and (2) quantifying configurational entropy contributions arising from Al and Si disorder on tetrahedral sites and from Mg and Al disorder on octahedral sites.

General aspects of the monoclinic amphibole crystal structure were discussed in detail by Hawthorne (1983) and specific implications of its structure on the interpretation of MAS NMR spectra were presented by Raudsepp et al. (1987) and Welch et al. (1994). As shown in Figure 1, there are two types of tetrahedral sites (T1 and T2) onto which a total of 8 Si + Al (per 24 O + OH) can substitute. In tremolite, the T1 and T2 sites have the nearest-neighbor cation environment of 3 and 2 Si, respectively, i.e., T1(Si_3) and T2(Si_2). There are three types of octahedral sites M1, M2, and M3 onto which a total of 5 Mg + Al cations can substitute (2 × M1, 2 × M2, and 1 × M3). Finally, there are 2 M4 sites, which are eight coordinated and ideally contain only Ca. As discussed at length in previous studies (Jenkins 1987; Graham et al. 1989), there is strong evidence supporting the stable substitution of 8–10% Mg for Ca on the M4 sites in synthetic tremolitic amphibole and that this level of substitution is maintained along the join under investigation (Jenkins 1994). This study was designed to investigate the distribution of Al among individual tetrahedral and octahedral sites with increasing Al content. Unlike previous MAS

* Present address: Department of Geology, Stanford University, Stanford, California, 94305, U.S.A.

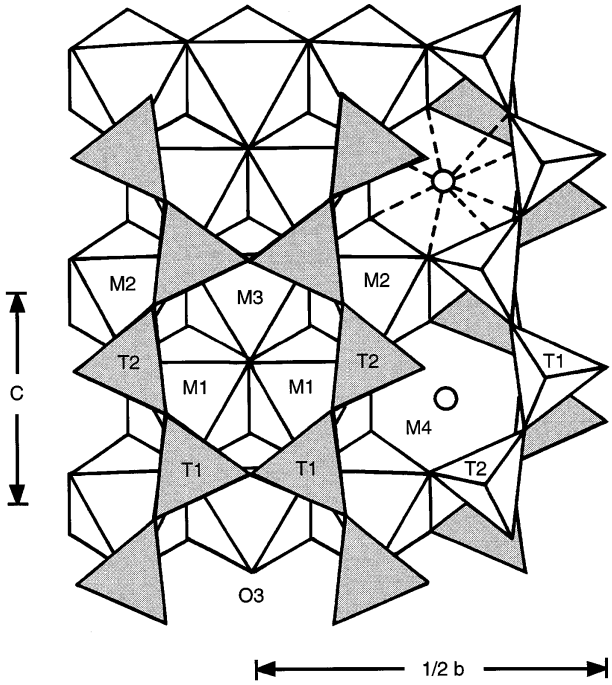

FIGURE 1. A portion of the crystal structure of *C*2/*m* amphibole projected onto the (100) axis (after Hawthorne 1983).

NMR studies which have dealt with the spectrum of a single amphibole (Smith et al. 1983; Mägi et al. 1984; Welch et al. 1994) or a series of chemically dissimilar amphiboles (Raudsepp et al. 1987), this study seeks to correlate changes in the MAS NMR spectra with changes in the Si, Al, and Mg contents related simply by the Tschermaks exchange.

The EMP analysis and Rietveld refinement of powder XRD data were used to characterize the experiment products. FTIR spectroscopy, along with ^{29}Si and ^{27}Al MAS NMR, were used to study the ordering of the tetrahedral and octahedral cations. With MAS NMR spectroscopy, different atomic environments can be detected, and therefore estimation of the occupancy is feasible. In addition, changes in peak width with composition can be used to characterize changes in the ordering throughout the series.

EXPERIMENTAL TECHNIQUES

Amphibole synthesis

A series of five amphiboles were synthesized at 830–875 °C and at 6–13 kbar along the join $Ca_{1.8}Mg_{5.2}Si_8O_{22}(OH)_2$-$Ca_{1.8}(Mg_{4.2}Al)(AlSi_7)O_{22}(OH)_2$ (approximately tremolite-magnesiohornblende) with end-members that are related by the Mg-Tschermaks exchange. Starting materials were prepared from mixtures of reagent grade $CaCO_3$, MgO, Al_2O_3, and SiO_2 (from desiccated silicic acid). Each mixture was roasted in air for 10–30 min at ~900 °C to drive off the CO_2 from $CaCO_3$ just before being sealed in either a gold or platinum capsule with 22–31 wt% water. The nominal compositions and synthesis conditions are given in Table 1. The most aluminous amphiboles (AMPH 19-7, 28-1, and 14-6) were synthesized at 13 kbar to obtain the maximum possible Al solubility in tremolitic amphibole (Jenkins 1988; Cho and Ernst 1991); accordingly, these syntheses experienced the greatest loss of silica to the ambient water during hydrothermal treatment (Jenkins 1987). Approximately 1.0 wt% additional quartz was mixed into these higher-pressure syntheses to compensate for this loss of silica to the ambient fluid.

Rietveld refinement from powder XRD data

Powder XRD patterns were obtained using a Scintag XDS-2000 diffractometer operated in the vertical θ-θ configuration using Cu radiation and a Si(Li) detector. Step scans were made over the range of 14–100° 2θ at 0.1° 2θ increments for a counting time of 1 s per step (500–1000 counts on maximum peaks) and using 2 mm primary and 0.3 mm receiving slits. The two lowest angle reflections were deleted owing to the relatively wide divergent slit used (beam area > sample area), which gave the lowest angle reflections abnormally low intensities. This does not significantly affect the results because the principal structural information retrieved from these refinements is the lattice parameters, which are more accurately defined by the higher-angle reflections. Refinements were performed using the program DBWS-9006 (Young 1993). Initially the powder patterns were refined as single-phase amphiboles to define various sample and instrumental parameters in a sequence identical to that used by Jenkins and Hawthorne (1995). Owing to the similarities in the X-ray scattering factors of Mg, Al, and Si no reasonable

TABLE 1. Nominal compositions, experiment conditions, and products of synthesis

Sample	Composition (Al total/23 O atoms)	*T* (°C)	*P* (kbar)	*t* (hrs)	Products*
TREM 23-5	$(Ca_{1.8}Mg_{0.2})Mg_5[Si_8O_{22}](OH)_2$ (0.0)	838(17)	6.1(1)	188	amph, [Cpx]
AMPH 25-1	$(Ca_{1.8}Mg_{0.2})(Mg_{4.6}Al_{0.4})[Al_{0.4}Si_{7.6}O_{22}](OH)_2$ (0.8)	875(10)	6.0(5)	109	amph
AMPH 19-7	$(Ca_{1.8}Mg_{0.2})(Mg_{4.4}Al_{0.6})[Al_{0.6}Si_{7.4}O_{22}](OH)_2$ (1.2)	830(5)	12.8(4)	144	amph, [Cpx], [Opx], [silica]
AMPH 28-1	$(Ca_{1.8}Mg_{0.2})(Mg_{4.2}Al_{0.8})[Al_{0.8}Si_{7.2}O_{22}](OH)_2$ (1.6)	845(5)	12.8(3)	162	amph, [silica]
AMPH 14-6	$(Ca_{1.8}Mg_{0.2})(Mg_4\ Al)[AlSi_7O_{22}](OH)_2$ (2.0)	846(5)	13.1(3)	145	amph, Cpx, cor, [silica]

Notes: Abbreviations: amph = amphibole; Cpx = clinopyroxene; cor = corundum; Opx = enstatitic orthopyroxene; silica = amorphous silica.
* Phases in brackets observed by optical or microprobe imaging, not on XRD pattern. Cpx and cor in AMPH 14-6 are present at 1.5 ± 0.4 and 1.0 ± 0.2 wt%, respectively.

refinement of their site occupancies was possible and, instead, their abundances were fixed to those of the nominal amphibole composition. Typical R_{Bragg} values were 0.08 for amphibole and whole-pattern goodness-of-fit values were 1.10. Final refinements included diopside and corundum as additional phases with all of their sample parameters, other than scale factors, fixed to those of amphibole in order to quantify the relative proportions of these extraneous phases by the Rietveld technique (Bish and Post 1993).

Electron microprobe analysis

The fine-grain amphibole particles were mounted in epoxy resin, polished and then analyzed using a CAMECA SX-50 EMP operating at 15 kV and 20 nA with a beam diameter of approximately 1 μm and counting times of 20 s. Matrix corrections were performed with the PAP procedure (Pouchou and Pichoir 1985). The standards used were olivine (Mg*K*α), diopside (Ca*K*α, Si*K*α), and kyanite (Al*K*α). Because of the small size of the amphibole fibres (generally 1–3 μm wide by 10–20 μm long) the electron-beam excitation volume frequently exceeded the crystal volume and produced low analytical totals. Therefore, an EMP analysis was deemed acceptable if the analytical totals were between 70–98 wt% and the mineral stoichiometry adhered closely to that of amphibole, i.e., cation totals were 15.0 ± 0.1 and Ca ≤ 2.0 on the (anhydrous) basis of 23 O apfu.

Fourier transform infrared spectroscopy

FTIR spectra were collected in the region of the main OH-stretching bands of 3500–3800 cm^{-1} using a Perkin-Elmer 1600 having a nominal resolution of 2 cm^{-1}. Samples were prepared by mixing 5–6 mg of the amphibole with 360 mg of KBr and pressing this under vacuum into a 12.7 mm diameter pellet. The FTIR spectra were referenced against a pure KBr pellet scanned at the same instrument conditions.

Nuclear magnetic resonance spectroscopy

MAS NMR spectra were obtained using a Doty high speed MAS probe with a Bruker AMX-500 multinuclear Fourier transform spectrometer. Powdered samples of the amphiboles were spun at speeds of between 6 and 8 kHz at an angle of 54.7° to the magnetic field. MAS NMR spectra for ^{29}Si were recorded at a frequency of 99.3 MHz with 8190 data points, a spectral width of 50 kHz, 30° pulses, and delays of between 5 and 300 s between pulses. The best signal-to-noise ratio for a given experimental time was obtained with a delay of 30 s, which was used for the spectra analyzed and displayed in this study. Spectra for ^{27}Al were recorded at a frequency of 130.3 MHz with a spectral width of 50 kHz, 10° pulses, and 0.1 s delay between pulses. Peak positions were measured with reference to tetramethylsilane (TMS) for ^{29}Si and a 1 *M* aqueous solution of aluminum chloride for ^{27}Al.

The relative intensities of the ^{29}Si spectral peaks were found by fitting peaks, with a combination of Gaussian and Lorentzian lineshapes, to the spectra using the least-squares deconvolution option in the Bruker NMR program UXNMR. The input parameters for the deconvolution were peak widths of 200 Hz and the position of the peaks. The program then adjusted the peak positions and widths over a series of iterations until a minimum was found. Initially peaks were placed at −82, −87, and −92 ppm with an additional peak at −107 ppm relating to the resonance envelop from −96 to −112 ppm for samples AMPH 19-7, AMPH 28-1, and AMPH 14-6. It was also possible to fit at least two peaks under each resonance in the spectra. We believe that these multiple peak fittings have less credibility than the three or four peak fits because there is no visible differentiation of the observed peaks. The relative intensities were calculated for the three peaks relating to Si within the structure of amphibole. However it should be noted that there may be a contribution from Opx and Cpx toward the peak at −84 ± 0.5 ppm.

^{27}Al has spin ½, therefore it has a large quadrupole moment for which quadrupole shifts in line position and intensities could be substantial (Lippmaa et al. 1986). Accordingly, the ^{27}Al spectra for AMPH 25-1, 19-7, and 28-1 were fitted by a least-squares technique, which modeled quadrupole line shapes (program kindly supplied by J.H. Baltisberger). The spectrum of AMPH 25-1 was fitted first as it has the best separation of the octahedrally coordinated peaks. The derived values for the quadrupole coupling constant (C_Q), asymmetry parameter (η), and isotropic chemical shift (δ_{iso}) were then entered as the initial values for fitting the other spectra, and the values were constrained within limits. The least-squares fitting program then iterated the values until a minimum was found. Because of the inaccuracies that would be introduced by the overlapping peak from corundum, the spectrum of AMPH 14-6 was not included in this fitting routine.

Results

Products of synthesis

The amphibole yields were high (97–99 wt%) with only traces of impurities visible under the petrographic microscope and in the XRD patterns. Diopsidic Cpx, Opx, and corundum were the only additional phases observed by optical, EMP, or XRD techniques (Table 1). Amorphous silica was observed in the MAS NMR spectra of the three highest pressure syntheses (AMPH 19-7, 28-1, and 14-6, Table 1). It probably occurs as a finely disseminated coating precipitated onto the surrounding grains from the aqueous fluid during the hydrothermal quench because it was never directly detected with optical or microprobe examination.

Electron microprobe analyses

Chemical compositions of the five amphibole samples calculated from averages of the EMP data are given in Table 2. Considering the large uncertainties associated with the analysis of these fine-grained fibers, there is gen-

TABLE 2. Average compositions of amphiboles from electron microprobe analysis expressed as cations/23 oxygen atoms

Cations	TREM 23-5	AMPH 25-1	AMPH 19-7	AMPH 28-1	AMPH 14-6
Si	8.0(1)	7.71(2)	7.34(4)	7.0(1)	7.1(1)
$^{[4]}$Al	0.0	0.29(2)	0.66(4)	1.0(1)	0.9(1)
$^{[6]}$Al	0.0	0.33(3)	0.64(3)	0.88(8)	0.94(3)
$^{[6]}$Mg	5.0(0)	4.67(3)	4.36(3)	4.11(8)	4.06(3)
$^{[8]}$Mg	0.2(2)	0.10(5)	0.16(7)	0.13(4)	0.1(1)
Ca	1.79(6)	1.88(3)	1.85(5)	1.91(2)	1.88(1)
Sum	14.99	14.98	15.01	15.03	14.99

Note: Uncertainty (1σ) in last digit shown in parentheses.

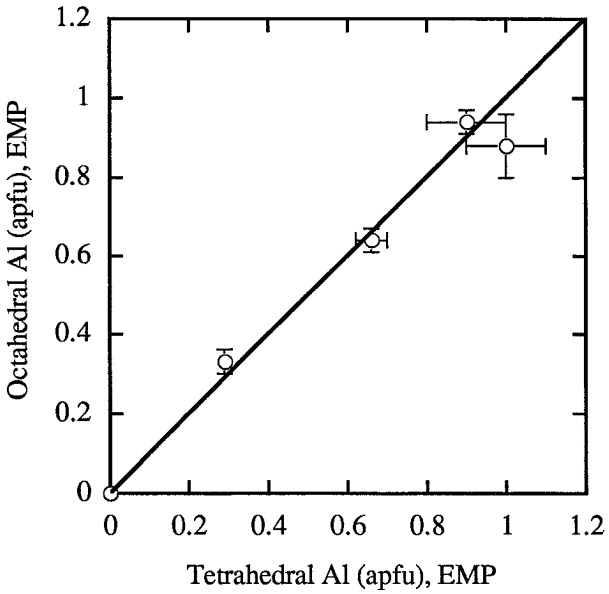

FIGURE 2. Octahedrally coordinated Al vs. tetrahedrally coordinated Al (apfu) from EMP analyses for amphiboles synthesized in this study. Solid diagonal line represents ideal one-to-one correspondence.

erally good agreement between the ideal and observed compositions. Notable exceptions are the high total Al content of AMPH 28-1 (1.88 observed vs. 1.6 ideal) and the low total Al of AMPH 14-6 (1.84 observed vs. 2.0 nominal). The discrepancy for AMPH 28-1 is not readily explained but the discrepancy for AMPH 14-6 is in agreement with the corundum observed in the synthesis products, indicating that the limit of Al solubility in tremolitic amphibole lies at about 1.9 apfu or just below the intended 2.0 apfu. A plot of $^{[6]}$Al vs. $^{[4]}$Al, as calculated from the EMP data, is shown in Figure 2 and follows the 1:1 correlation line closely. This indicates that Al is equally distributed between these environments and demonstrates that the Tschermak's substitution is closely obeyed.

Rietveld refinements

The unit-cell dimensions are listed in Table 3 and are plotted against the total Al content (apfu) as determined from the EMP results (Fig. 3). There is a systematic decrease in unit-cell volume in response to the Tschermaks substitution, which is consistent with this substitution into pyroxenes (Skinner and Boyd 1964; Newton et al. 1977) and an earlier study of aluminous tremolite (Smelik et al. 1994). Notice that the volume reduction occurs despite an increase in the *c* dimension showing that volume reduction is dominated by reductions in the *a* and *b* dimensions and in sinβ. Also notice that the most aluminous amphibole (AMPH 14-6) has unit-cell dimensions that are very similar to the next most aluminous sample, reaffirming that AMPH 14-6 does not have a full 2.0 Al apfu. It was not possible to detect changes in interatomic distances with the substitution of Al into the structure, owing to the relatively low precision in the atomic positions refined in this technique. It is noted that the refined structures produced interatomic distances that were commensurate (within 0.02 Å) with those from single-crystal structure analyses of tremolitic amphiboles (Papike et al. 1969).

Determination of the relative proportions of amphibole, diopsidic Cpx, and corundum by the Rietveld technique indicated that only the most aluminous sample (AMPH 14-6) had quantifiable amounts of these phases, which were 1.5 ± 0.4 wt% Cpx and 1.0 ± 0.2 wt% corundum. Assuming to a first approximation that all of the Al not incorporated into amphibole resides in corundum (Cpx has only ≈ 6 wt% Al_2O_3), one can calculate the maximum amount of Al that could be incorporated into the amphibole. This is simply the difference between the bulk Al_2O_3 of the starting mixture (12.6 wt%) less 1.0 ± 0.2 wt% in corundum or 11.6 ± 0.2 wt% Al_2O_3. This corresponds to a maximum of 1.8 ± 0.2 Al total apfu, which is the same as that observed from the microprobe analysis (1.8 ± 0.1 Al apfu), and lends support to the general accuracy of our assessment of the Al contents in the synthetic amphiboles.

TABLE 3. Unit-cell parameters for amphibole (*C*2/*m*) synthesized in this study

	TREM 23-5	AMPH 25-1	AMPH 19-7	AMPH 28-1	AMPH 14-6
a(Å)	9.807(2)	9.784(1)	9.779(1)	9.768(1)	9.762(1)
b(Å)	18.054(3)	18.027(2)	18.013(2)	17.990(2)	17.987(2)
c(Å)	5.2765(8)	5.2795(5)	5.2851(6)	5.2877(6)	5.2899(6)
β(°)	104.56(1)	104.741(6)	104.829(8)	104.910(7)	104.926(8)
V(Å^3)	904.2(2)	900.6(2)	900.0(2)	897.9(2)	897.5(2)

Note: Uncertainty in last digit shown in parentheses.

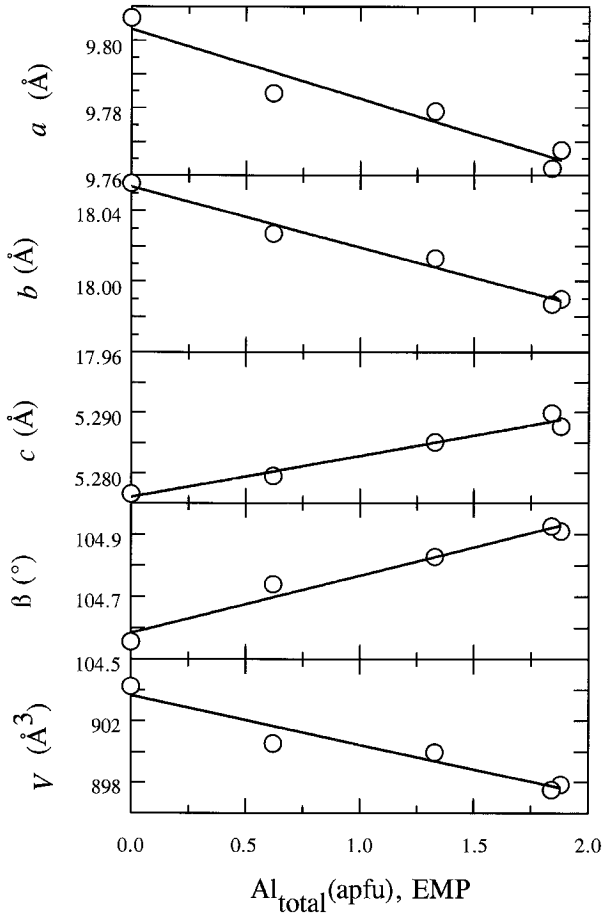

FIGURE 3. Unit-cell parameters *a*, *b*, *c*, β, and volume vs. total Al cations (apfu) from EMP analysis for amphiboles synthesized in this study. Solid lines represent linear least squares best fit to the data.

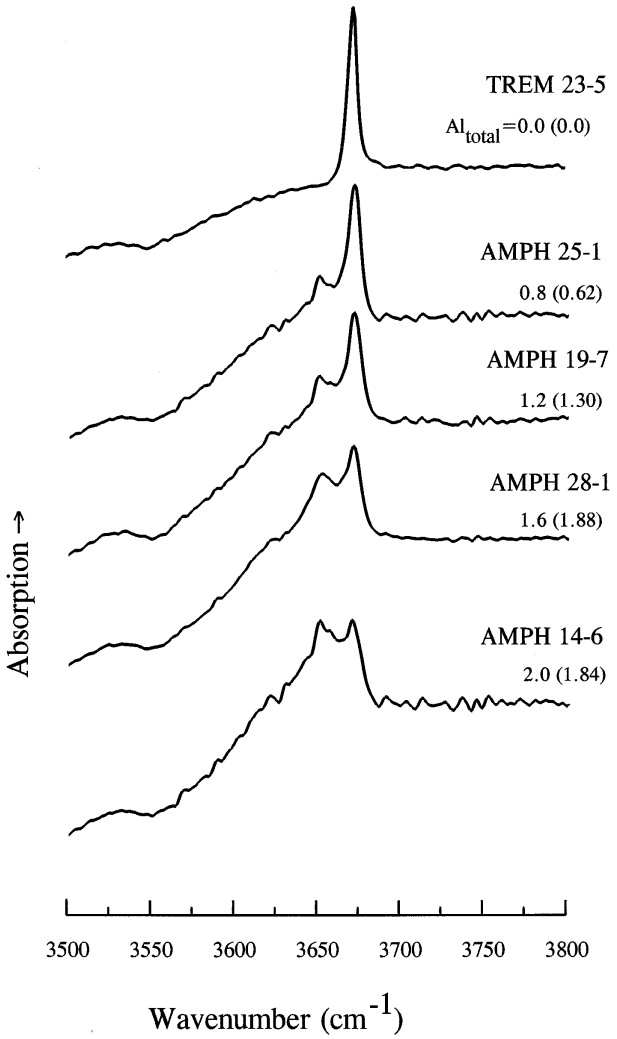

FIGURE 4. FTIR spectra of the five synthetic amphiboles. Nominal (and observed) total Al apfu are indicated.

Fourier transform infrared spectroscopy

The FTIR spectra of the amphiboles are shown in Figure 4 ranked in order of increasing total Al. The Al-free sample (TREM 23-5) shows a single sharp band at 3672 cm^{-1} with a full-width at half-maximum (FWHM) of ~7 cm^{-1}. This band has long been documented as the (MgMgMg)-OH-stretching vibration for tremolite (Burns and Strens 1966), which arises from the bonding of OH at the O(3) site with three nearest neighbour octahedral cations, 2 M1 and 1 M3. In tremolite these sites are occupied by Mg and have identical configurations around the OH, producing a single sharp band. As the Al content is increased the relative intensity of the (MgMgMg)-OH band decreases and a band at 3652 cm^{-1} appears. This latter band increases in relative intensity with increasing Al content with little shift in position. It never appears in these spectra so sharply or well resolved as the (MgMgMg)-OH band making the determination of the FWHM difficult. This band is attributed here to Al substitution into either the M3 or one of the M1 positions to produce an MgMgAl configuration around the OH and an associated lower-frequency band. According to the single-crystal structural refinement study by Oberti et al. (1995b), one would attribute this band to Al on the M3 and not the M1 site. If Al only substituted onto the M2 site, as is commonly deduced from crystallographic studies (Hawthorne 1983), there should only be one band [the (MgMgMg)-OH] because OH is not directly bonded to the M2 cation.

The position of the (MgMgAl)-OH band observed here is shifted −20 cm^{-1} from that of the (MgMgMg)-OH band. Although the direction of shift agrees with what one would predict from the substitution of the more electronegative Al (1.47) for Mg (1.23), the magnitude of the shift is considerably greater than the −9 cm^{-1} predicted from the relationship given by Strens (1974). This same behavior was noted for pargasite by Raudsepp et al. (1987) who observed a major band shifted −33 cm^{-1} from the (MgMgMg)-OH-Na band of pargasite, which they attributed to an (MgMgAl)-OH-Na band. The band

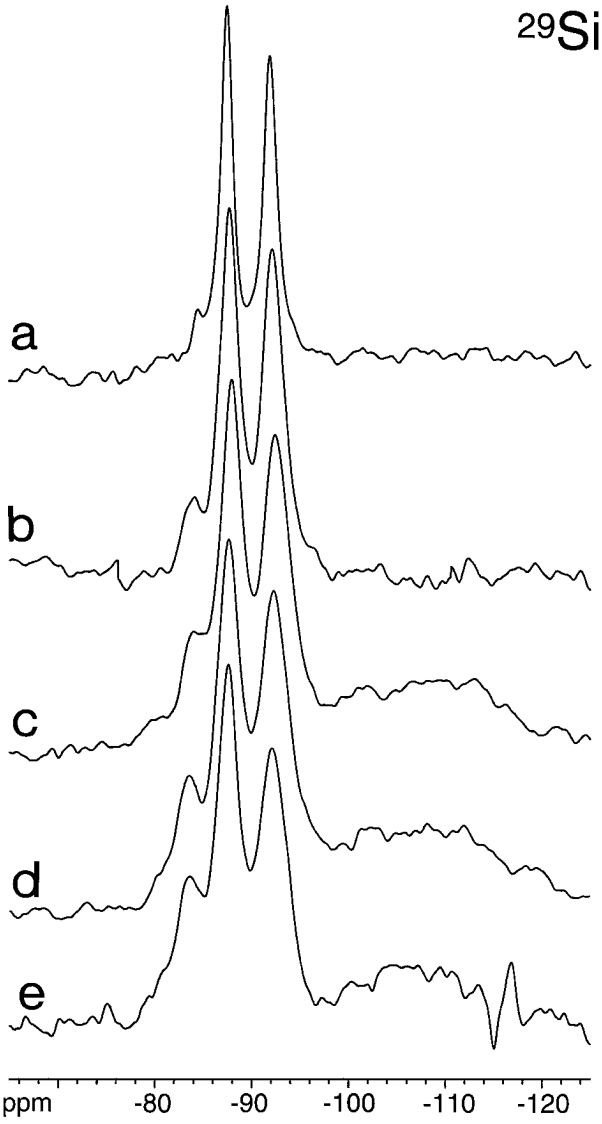

FIGURE 5. ^{29}Si MAS NMR spectra of $^{[4]}$Si in (**a**) TREM 23-5, (**b**) AMPH 25-1, (**c**) AMPH 19-7, (**d**) AMPH 28-1, and (**e**) AMPH 14-6.

observed here at 3652 cm^{-1} is in very close agreement with the MgMgAl band at 3654 cm^{-1} (band K) reported by Bancroft and Burns (1969) for A-site absent alkali amphiboles, again supporting its assignment as an (MgMgAl)-OH vibration.

The appearance of only one extra lower-wavenumber OH-stretching band with the addition of Al is in agreement with the bond-valence analysis recently presented by Hawthorne (1995). Hawthorne (1995) argued that the presence of two or more Al cations coordinated to the OH at the O(3) position produces a bond-valence excess at the OH anion that cannot be accommodated by structural relaxation. Accordingly, one would not expect an (MgAlAl)-OH or (AlAlAl)-OH band to appear.

TABLE 4. Relative intensities of ^{29}Si NMR peaks

Sample code (other phases)*	$^{[4]}$Al apfu**	Peak position (ppm)	Peak width (Hz)	Area	Relative intensity (%)
TREM 23-5	0	−84.5	130	33	4
(Cpx)		−87.5	143	356	48
		−92.0	169	363	48
AMPH 25-1	0.3	−83.8	145	47	5
		−87.7	210	440	47
		−92.3	236	449	48
AMPH 19-7	0.7	−83.8	228	127	9
(Cpx, Opx, silica)		−87.8	241	587	44
		−92.5	303	636	47
		−109	1410	689	
AMPH 28-1	1.0	−83.4	206	32	10
(silica)		−87.6	259	141	42
		−92.5	349	162	48
		−106	1690	235	
AMPH 14-6	0.9	−83.4	352	290	21
(Cpx, Opx, silica)		−87.6	252	570	41
		−92.3	301	544	39
		−107	1520	697	

* Phase abbreviations as in Table 1.
** These values are calculated from the electron microprobe analyses.

Nuclear magnetic resonance spectroscopy

^{29}Si MAS NMR. The ^{29}Si MAS NMR spectrum of synthetic tremolite, sample TREM 23-5, consists of two peaks of equal intensity at −87 and −92 ppm (Fig. 5a). Peaks with the same chemical shifts were allocated to Si in the T2(Si_2) and T1(Si_3) environment, respectively (Smith et al. 1983; Raudsepp et al. 1987). The peaks in our spectrum of tremolite are much narrower and better resolved than in previously published spectra of natural tremolite (Smith et al. 1983; Raudsepp et al. 1987) or synthetic pargasite (Welch et al. 1994). This change may reflect the absence of aluminum in this sample, which eliminates any broadening because of Al-Si disorder or quadrupole-dipole coupling between ^{29}Si and ^{27}Al, or the absence of paramagnetic ions, which, in the sample studied by Raudsepp et al. (1987), are present at a level of 0.11 wt% (FeO + MnO). The small peak at −84 ppm in this spectrum is interpreted as being caused by ^{29}Si in Cpx (Smith et al. 1983), present in trace amounts in this sample (Table 1).

The peaks at −87 and −92 ppm, which are present in the spectra of all the aluminous-tremolite samples (Fig. 5b–e), broaden systematically with increasing Al content in the amphiboles (Table 4). The peak at −84 ppm is broader in the spectra of AMPH 19-7 and 14-6 (Fig. 5c and 5e) than for the other samples. This is interpreted as resulting from overlapping peaks from the amphibole and from Cpx and Opx impurities at −84 and −80 ppm, respectively (Smith et al. 1983). The relative intensity of the peak at −84 ppm increases as the intensity of the peak at −87 ppm decreases systematically with increasing Al content for samples AMPH 25-1, AMPH 19-7, and AMPH 28-1 (Table 4). The relative intensity of the peak at −92 ppm apparently remains unchanged. In the spectrum of AMPH 14-6 the peak at −83 ppm accounts for 21% of the total spectral intensity with a simultaneous

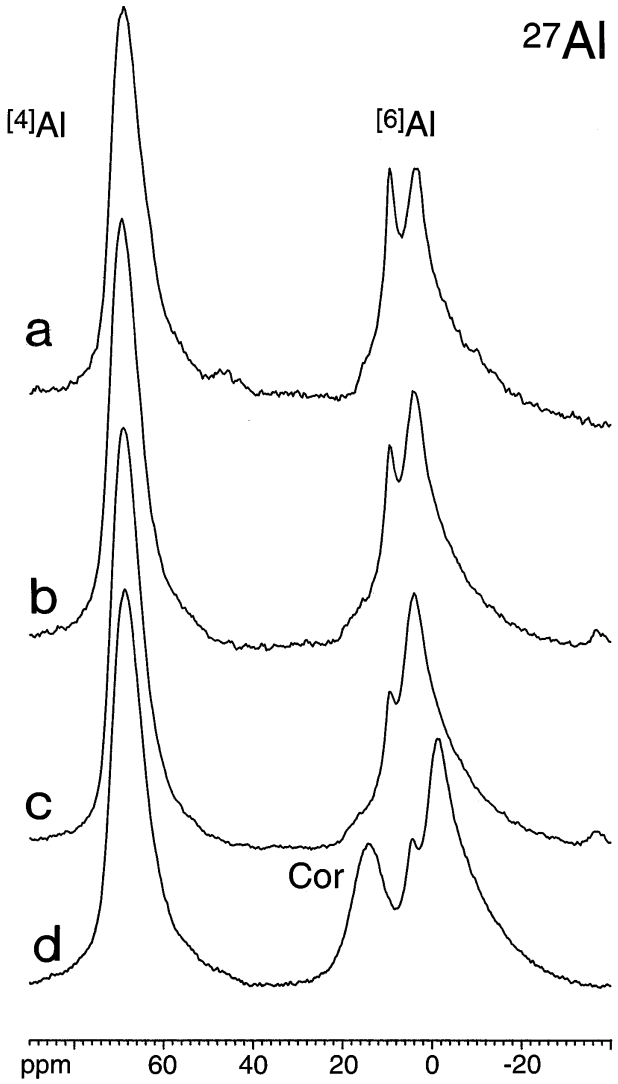

FIGURE 6. ^{27}Al MAS NMR spectra of $^{[4]}$Al and $^{[6]}$Al in (**a**) AMPH 25-1, (**b**) AMPH 19-7, (**c**) AMPH 28-1, and (**d**) AMPH 14-6; the peak at 13 ppm is because of an impurity of corundum (Cor).

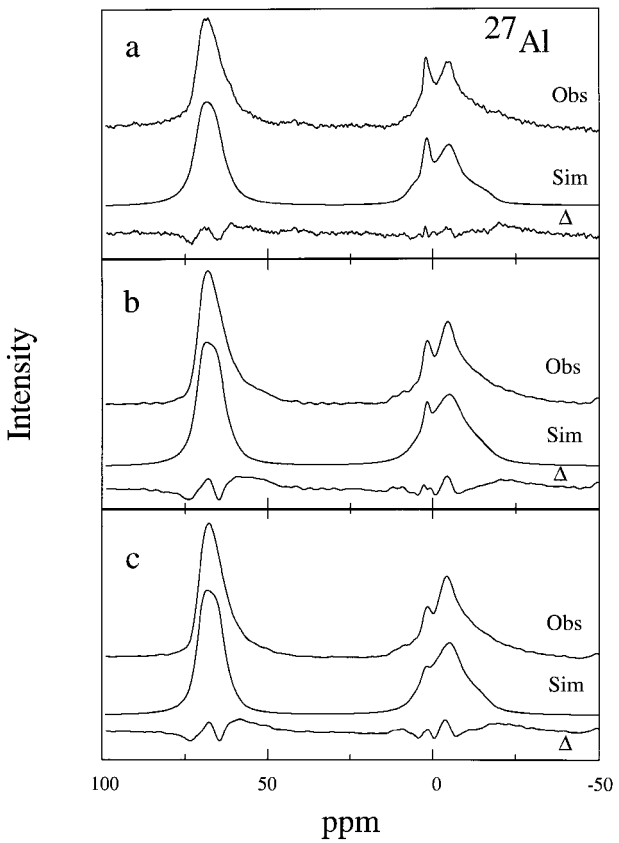

FIGURE 7. Observed (Obs) and simulated (Sim) MAS NMR ^{27}Al MAS NMR spectra for (**a**) AMPH 25-1, (**b**) AMPH 19-7, and (**c**) AMPH 28-1 from Fig. 6. Difference between the observed and simulated spectra is shown by the curve labelled Δ.

reduction of the intensity of the peak at −92 ppm. These relative intensities may be distorted by the relatively large amounts of Cpx, corundum, and amorphous Si in this sample.

There is also a broad resonance from −95 to −120 ppm in the spectra of AMPH 19-7, 28-1 and 14-6 (Fig. 5c, d, and e). This width of peak is similar to those from glasses (Sherriff and Fleet 1990; Stebbins et al. 1995) and therefore is interpreted as amorphous silica that was probably precipitated over the grains as a fine coating during the quench. Peaks, with widths between 1400 and 1700 Hz, were fitted to these envelopes but the intensity was not included in the calculation of relative intensities (Table 4).

^{27}Al MAS NMR. There are three peaks in the ^{27}Al MAS NMR spectra of aluminous tremolite as shown in Figure 6. The refined values of C_Q, η, and δ_{iso} as well as the relative intensities for the peaks corrected for quadrupolar effects are listed in Table 5 and the corresponding simulated spectra are shown in Figure 7. The prominent peak at 13 ppm in AMPH 14-6 (Fig. 6d) is attributed to minor corundum, similar to the spectra observed for synthetic phlogopitic mica by Circone et al. (1991). The small peak at 45 ppm in the spectrum of AMPH 25-1 (Fig. 6a) is a spinning sideband of a peak at 103 ppm because of an impurity in the rotor.

The peak at 68.7 to 67.2 ppm, referred to here as the 68 ppm peak, is due to tetrahedrally coordinated Al in either the T1 or T2 sites. The results of the spectral fittings (Table 5, Fig. 7) show an increase in the asymmetry parameter, η, with increasing Al content as well as a slight increase in quadrupole coupling constant C_Q from 3.6 to 3.7 MHz. This could be because of a distortion of the lattice with Al entering both the octahedral and tetrahedral sites. There is a slight shift of the isotropic chemical shift (δ_{iso}) to higher field with increasing Al content from 71.8 ppm for AMPH 25-1 to 71.5 ppm for AMPH 28-1. It is not possible to determine solely from the ^{27}Al

TABLE 5. ^{27}Al NMR spectral fitting parameters and relative intensities

	Sample code		
	AMPH 25-1	AMPH 19-7	AMPH 28-1
Total Al (apfu) from EMP	0.6	1.3	1.9
68 ppm peak			
η	0.0	0.0	0.1
C_Q (MHz)	3.6	3.7	3.7
δ_{iso} (ppm)	71.8	71.7	71.5
Relative intensity	55%	51%	53%
$^{[4]}$Al (apfu) from NMR	0.34	0.67	0.99
$^{[4]}$Al (apfu) from EMP	0.29	0.66	1.0
3 ppm peak			
η	0.0	0.0	0.2
C_Q (MHz)	0.0	0.2	0.5
δ_{iso} (ppm)	3.3	3.3	3.7
Relative intensity	3%	1%	1%
$^{[6]}$Al (apfu) from NMR	0.02	0.02	0.01
−2 ppm peak			
η	1.0	1.0	1.0
C_Q (MHz)	4.9	4.6	4.6
δ_{iso} (ppm)	8.7	7.0	6.7
Relative intensity	42%	47%	47%
$^{[6]}$Al (apfu) from NMR	0.26	0.61	0.88
Total $^{[6]}$Al (apfu) from NMR	0.28	0.63	0.89
Total $^{[6]}$Al (apfu) from EMP	0.33	0.64	0.88

NMR spectra how Al is partitioned between the T1 and T2 sites.

There are two octahedrally coordinated peaks; one varying from 2.8 to 4.2 ppm, referred to here as the 3 ppm peak, and one varying from −1.8 to −2.8 ppm, referred to here as the −2 ppm peak. The relative intensity of the −2 ppm peak increases steadily with increasing Al content in the amphibole (Fig. 6 a–6d). The number of Al atoms per formula unit in each site were calculated from the total Al content determined by means of EMP analysis and the relative intensities of the fitted peaks. As seen in Table 5, the Al content of the −2 ppm peak increases markedly from 0.26 to 0.88 apfu while the 3 ppm peak remains low at about 0.02 apfu. It should be noted that the total $^{[4]}$Al and $^{[6]}$Al deduced from NMR data are in close agreement with each other, which reinforces the EMP data that the Tschermaks substitution is obeyed.

DISCUSSION

Si-Al ordering in the tetrahedral sites

The allocation of the peaks to environments in the amphibole structure is somewhat controversial. Peaks at −87 and −92 ppm have previously been allocated to Si in T2(Si_2) and T1(Si_3) environments respectively (Smith et al. 1983). With the addition of Al one would expect additional peaks because of T2(SiAl), T1(Si_2Al) and T1($SiAl_2$) environments to appear. The exchange of a neighbouring Si atom by an Al atom would give a ^{29}Si chemical shift to low field of about 4 ppm when estimated using the method developed by Sherriff et al. (1991). This is only an estimate, however, because exact positions of neighbouring atoms are required for the calculation and in this case the T-site atomic positions, obtained from the structural refinement of XRD data, are an average of Si- and Al-containing tetrahedra. One interpretation would be that the peak at −84 ppm is due to T2(SiAl) and possibly T1($SiAl_2$), and that the peak at −87 ppm contains overlapping peaks from T2(Si_2) and T1(Si_2Al). Another interpretation is that the intensity from T1(Si_2Al) contributes toward the peak at −92 ppm and that from T1($SiAl_2$) to the −87 ppm peak. Attempts were made experimentally to resolve separate peaks under both the −87 and −92 ppm peaks by reducing the exponential line broadening but without success. It is possible, with the least squares deconvolution program, to fit two or more peaks under each of the three measured resonances but the resultant spectra gave singularities in the shapes of the peaks that were not present in the experimental data.

TABLE 6. Calculated relative intensities of ^{29}Si NMR peaks (Si site occupancies apfu)

Al (apfu)	Si site environments			
	T2(SiAl)	T2(Si_2)	T1(Si_2Al)	T1(Si_3)
Al in T1 site only				
0.0	—	50% (4.0)	—	50% (4.0)
0.3	8% (0.6)	44% (3.4)	4% (0.3)	44% (3.4)
0.6	16% (1.2)	38% (2.8)	8% (0.6)	38% (2.8)
1.0	29% (2.0)	29% (2.0)	14% (1.0)	29% (2.0)
Al in T2 site only				
0.3	—	48% (3.7)	8% (0.6)	44% (3.4)
0.6	—	46% (3.4)	16% (1.2)	38% (2.8)
1.0	—	43% (3.0)	29% (2.0)	29% (2.0)
Al in both T1 and T2				
0.15	4% (0.3)	46% (3.55)	6% (0.45)	44% (3.4)
0.3	8% (0.6)	42% (3.1)	12% (0.9)	38% (2.8)
0.5	14% (1.0)	36% (2.5)	21% (1.5)	29% (2.0)

The effect that distributing Al between the two tetrahedrally coordinated sites would have on the ^{29}Si spectra was calculated for incremental amounts of Al entering either the T1, T2, or being evenly distributed between the two sites (Table 6). Each Al atom entering a T1 site would reduce the population of the T1(Si_3) site by two as one adjacent T1 site would become a T1(Si_2Al) environment. It would also cause the environment of two adjacent T2 atoms to change from T2(Si_2) to T2(SiAl). One Al atom entering the T2 site would reduce the population of the T2 site by one and cause two adjacent T1(Si_3) environments to become T1(Si_2Al).

Amphiboles AMPH 25-1 (0.3 $^{[4]}$Al) and AMPH 28-1 (1.0 $^{[4]}$Al) have apparently no visible impurities of Cpx and Opx (Table 1) to distort the relative intensities of the −84 ppm peak; therefore, these samples were used to compare calculated and experimental relative intensities. The relative intensity of the −84 ppm peak for these two compositions is 5% and 10%, respectively. The calculations in Table 6 show that Al must be put into the T1 site to provide Si in the T2(SiAl) environment, which would produce the ^{29}Si experimental peak at −84 ppm. However if all the tetrahedral Al entered the T1 site this peak would represent 8% and 29% of the relative intensity of the spectra for AMPH 25-1 and 28-1, respectively. If $^{[4]}$Al

is evenly distributed between the T1 and T2 sites the relative intensities of the T2(SiAl) peaks will be 4% and 14% for AMPH 25-1 and 28-1, respectively, which is much closer to the experimental values (Table 4) and indicates that Al is randomly distributed over both the T1 and T2 sites.

Because the peak due to the T1(Si_2Al) is not resolved separately it can contribute to either or to both of the resonances at −87 and −92 ppm. This fact would explain the increase in peak widths with Al content. However as the peak intensity of the −92 ppm peak remains at 48% (except for AMPH 14-6) and the peak width increases at a greater rate, it would seem that the intensity because of T1(Si_2Al) is contributing more to the −92 ppm peak than to the −87 ppm peak. If the calculated relative intensities of the T1(Si_2Al) and T1(Si_3) are combined for the scenario of having Al equally distributed between the two T sites, the relative intensities for the three peaks for 0.3 and 1.0 $^{[4]}$Al apfu are 4:46:50 and 14:36:50, respectively, which compare favorably to the measured relative intensities for AMPH 25-1 and 28-1 of 5:47:48 and 10:42:48. The experimental ratios could be obtained by putting more than 50% of the Al in T2 in the case of AMPH 25-1 and less than 50% for AMPH 28-1; however, given the error inherent in measuring the relative intensities from fitting peaks to the spectra, we do not feel that further fine tuning of these calculations is meaningful.

Our interpretation of the ^{29}Si MAS NMR spectra is that Al is distributed between the two tetrahedral sites in aluminous tremolite. Because of the small amount of Al involved, the Al-O-Al avoidance rule (Lowenstein 1954) can be obeyed for all scenarios. Evidence for the temperature-induced disordering of $^{[4]}$Al over both the T1 and T2 sites in natural calcic amphiboles was recently given by Oberti et al. (1995a). Similarly, direct X-ray refinement of Ga (proxy for Al) on the T2 as well as T1 sites was reported by Jenkins and Hawthorne (1995) in gallian fluor-pargasites.

Al-Mg ordering in octahedral sites

The presence of Al on two different octahedral sites was confirmed in this study by the presence of two distinct peaks on the MAS spectra for ^{27}Al (Fig. 6). The assignment of these peaks to the M1, M2, and M3 octahedral sites is problematic because of the paucity of information about such correlations (Smith 1993). Accordingly, we offer the following two alternative interpretations of the ^{27}Al NMR spectra.

Kunath-Fandrei et al. (1995), in their correlation of the four peaks in their ^{27}Al spectrum of $Al_2(MoO_4)_3$ with four octahedral sites, show that the quadrupolar coupling constant (C_Q) is more sensitive to differences in distortion of the AlO_6 octahedra than the isotropic chemical shift. Using single-crystal NMR data, Ghose and Tsang (1973) found a better relationship between the quadrupolar coupling constant and the longitudinal strain (α) for octahedrally coordinated Al than for the shear strain (Ψ). The longitudinal strain is calculated as $\alpha = \Sigma|\ln(l_i/l_m)|$ with l_i and l_m being the individual and mean cation-oxygen bond lengths, respectively, and the shear (angular) strain is calculated from $\psi = \Sigma|\tan\theta_i - \tan\theta_0|$ where θ_i are the individual O-Al-O bond angles and θ_0 is the ideal bond angle (90°) for an octahedron. Averaging the single-crystal data for tremolite from Papike et al. (1969) and Hawthorne and Grundy (1976), one calculates values of α for M1, M2, and M3 sites of 0.021, 0.120, and 0.024, respectively, and those of ψ as being 1.16, 0.79, and 1.33. Although the shear strain is lowest for the M2 site the longitudinal strain is highest for the M2 site that, according to Ghose and Tsang (1973), would correlate with the NMR peak with the highest C_Q (−2 ppm). Calculation of the α parameters for the samples studied here is hindered by the inherently lower precision obtained for atomic coordinates from Rietveld analyses (Raudsepp et al. 1990). For synthetic tremolite (TREM 23-5) the α values are 0.08, 0.11, and 0.03 for the M1, M2, and M3 sites, respectively. Similar α values are obtained for the aluminous tremolites, with the M1 and M2 values both being about 0.08, the M3 about 0.04, and no obvious variation in α values for any site with increasing Al content. Until more precise crystallographic data are available for synthetic aluminous tremolite, one can only realistically use the single-crystal data for tremolite to estimate the octahedral-site distortions in our samples.

Assignment of the −2 ppm MAS NMR peak to the M2 site and the 3 ppm peak to the M1-M3 site is in general agreement with recent studies of amphibole crystal chemistry. X-ray diffraction evidence for disordering of octahedral Al or other $^{[6]}R^{3+}$ cations in OH-bearing amphiboles (not F-bearing) was presented for synthetic scandian pargasite by Raudsepp et al. (1987) and for natural pargasitic amphiboles from the Finero, Italy, complex by Oberti et al. (1995b). Welch et al. (1994) presented MAS NMR and cross-polarization MAS NMR data for synthetic pargasite. As in the present study, Welch et al. (1994) observed two octahedrally coordinated peaks in the ^{27}Al spectra. They showed that the narrow, less shielded peak at 8.4 ppm could be cross polarized with H from the OH group that is adjacent to the M1 and M3 sites. The broader and more shielded peak at −5 ppm did not cross polarize and they assigned this to the M2 site. Although the absolute positions of their octahedral peaks are not identical to those in this study, reflecting the different field strength of the two spectrometers and possibly differences in the host structures, the line widths and relative positions are similar, suggesting similar distributions of $^{[6]}$Al between synthetic (OH-bearing) tremolitic and pargasitic amphiboles. However, there can be problems in ensuring complete cross-polarisation with the broad resonances of quadrupolar nuclei such as ^{27}Al.

The analysis presented above hinges on the assumptions that (1) the direct relationship between C_Q and α established by Ghose and Tsang (1973) for octahedral Al is applicable to amphiboles and (2) that the octahedral site distortions of synthetic aluminous tremolites are accurately modelled by those of natural tremolite; both as-

sumptions have a considerable margin of doubt. It is noted, for example, that Ghose and Tsang (1973) discounted corundum, chrysoberyl (Al_2 site), and spodumene (the only chain silicate considered) from their analysis as being anomalous.

In contrast, the NMR chemical shifts and the relative IR band intensities can be used to support the reverse peak assignments. There are very few studies of the correlation of the isotropic chemical shift of Al in octahedral sites, except for the aluminum-silicate polymorphs, which do not have complicating factors of cation disorder (Xu and Sherriff 1993). It is difficult to obtain accurate quadrupolar shifts from powder pattern spectra of minerals with multiple octahedral sites and hence to be able to calculate the isotropic chemical shift from the peak positions. One major difference between the octahedral sites in amphiboles is that the M1 and M3 sites are coordinated to five O atoms and one OH group, whereas the M2 group is coordinated to 6 O atoms. The effect of the H atom should be to deshield the Al and produce a more positive value of isotropic chemical shift. When the large quadrupole shift of the −2 ppm peak is taken into consideration, the isotropic shift of this peak becomes more positive than the 3 ppm peak. This positive shift indicates that the −2 ppm peak should be allocated to the M1 and M3 sites and not the 3 ppm peak as indicated from the quadrupole coupling argument.

The presence of $^{[6]}$Al in the M1-M3 sites in all of the aluminous samples is corroborated by their FTIR spectra, which display an absorption band that correlates with Al in the M1-M3 sites (Fig. 4). Considering the FTIR and NMR spectra together, it appears that Al is disordered over both the M1-M3 and M2 sites at the very onset of the Tschermaks substitution into tremolitic amphibole. With increasing Al content, the FTIR spectra indicate that the Al occupancy in the M1-M3 site increases steadily, as evidenced by the increase in the 3652 cm^{-1} band intensity. This increase directly correlates with the −2 ppm ^{27}Al NMR peak, whose intensity also increases with increasing Al content, suggesting that it is because of Al in the M1-M3 sites. Unfortunately, this has the effect of placing the majority of octahedral Al on the M1-M3 sites (Table 5), which does not agree with most X-ray crystallographic studies (Hawthorne 1983; Makino and Tomita 1989; Oberti et al. 1995b).

Choosing between these two contrasting interpretations of NMR peak assignments will require, at the very least, further investigation into the correlation of C_Q and δ_{iso} with octahedral site distortion and shielding as well as a more precise determination of the octahedral site geometry in aluminous tremolitic amphiboles.

Finally, we note that substituting one Al for Mg in an octahedral site would cause a ^{29}Si peak shift of less than 1 ppm, to low field, for Si in an adjacent tetrahedral site (Sherriff et al. 1991). As these peaks are not separately resolved in the spectrum the effect could add to the broadening of the Si peak with increasing Al content (Table 4). Because the T1 site is adjacent to three octahedral sites (M1, M2, and M3) and the T2 site adjacent to only two octahedral sites (M1 and M2; Fig. 1), increasing the amount of Al in the octahedral sites should have a greater effect on the peak width of the Si T1 peak at −92 ppm than the Si T2 peak at −87 ppm. This agrees with our observations (Table 4).

Impurities

The relative intensities of NMR peaks from different minerals within a mixture cannot be used to determine the proportions of each phase present as the nuclear relaxation rates will be different for each phase. The relaxation rate of silica in a disordered state was shown to be faster than in ordered crystalline material (Hartman et al. 1987). Therefore the relatively large intensity of the broad resonance from −100 to −120 ppm in the ^{29}Si spectrum may be because of a relatively small amount of amorphous silica. Similarly the intensities of the Cpx and Opx peaks may be either enhanced or reduced relative to the amphibole, owing to differences in relaxation rates. It was not possible for the relaxation rates of these phases to be determined because a minimum delay of 30 s was required between pulses to be able to obtain spectra with good signal-to-noise ratios. This slow relaxation is typical of synthetic minerals that do not have trace impurities of transition metals to provide paramagnetic centers for efficient relaxation.

Acknowledgments

We wish to acknowledge the help of Kirk Marat and Terry Wolowiec with the NMR spectroscopy, Dave Teertstra and Ron Chapman for help collecting the electron microprobe data and Janice Liwanag for help with the figures. This research was funded by NSF grant EAR-9316079 to D.M.J. and an NSERC operating grant and University Research Fellowship Award to B.L.S. We greatly appreciate the comments of Mark Welch, Gary Ernst, and two anonymous reviewers whose comments substantially improved the manuscript.

References cited

Bancroft, G.M., and Burns, R.G. (1969) Mössbauer and absorption spectral study of alkali amphiboles. Mineralogical Society of America Special Paper, 2, 137–148.

Bish, D.L., and Post, J.E. (1993) Quantitative mineralogical analysis using the Rietveld full-pattern fitting method. American Mineralogist, 78, 932–940.

Burns, R.G., and Strens, R.G.J. (1966) Infrared study of the hydroxyl bands in clinoamphiboles. Science, 153, 890–892.

Cho, M., and Ernst, W.G. (1991) An experimental determination of calcic amphibole solid solution along the join tremolite-Tschermakite. American Mineralogist, 76, 985–1001.

Circone, S., Navrotsky, A., Kirkpatrick, R.J., and Graham, C. M. (1991) Substitution of $^{[6,4]}$Al in phlogopite: Mica characterization, unit-cell variation, ^{27}Al and ^{29}Si MAS-NMR spectroscopy, and Al-Si distribution in the tetrahedral sheet. American Mineralogist, 76, 1485–1501.

Ghose, S., and Tsang, T. (1973) Structural dependence of quadrupole coupling constant e^2qQ/h for ^{27}Al and crystal field parameter D for Fe^{3+} in aluminosilicates. American Mineralogist, 58, 748–755.

Graham, C.M., Maresch, W.V., Welch, M.D., and Pawley, A.R. (1989) Experimental studies on a amphiboles: A review with thermodynamic perspectives. European Journal of Mineralogy, 1, 535–555.

Hartman, J.S., Richardson, M.F., Sherriff, B.L., and Winsborrow, B.G. (1987) Magic angle spinning NMR studies of silicon carbide; polytypes, impurities and highly inefficient spin-lattice relaxation. Journal of the American Chemical Society, 109, 6059–6067.

Hawthorne, F.C. (1983) The crystal chemistry of the amphiboles. Canadian Mineralogist, 21, 173–480.

——— (1995) A multinuclear NMR study of synthetic pargasite—Discussion. American Mineralogist, 80, 628–629.

Hawthorne, F.C., and Grundy, H.D. (1976) The crystal chemistry of the amphiboles: IV. X-ray and neutron refinements of the crystal structure of tremolite. Canadian Mineralogist, 14, 334–345.

Jenkins, D.M. (1987) Synthesis and characterization of tremolite in the system H_2O-CaO-MgO-SiO_2. American Mineralogist, 72, 707–715.

——— (1988) Experimental study of the join tremolite-Tschermakite: A reinvestigation. Contributions to Mineralogy and Petrology, 99, 392–400.

——— (1994) Experimental reversal of the aluminum content in tremolitic amphiboles in the system H_2O-CaO-MgO-Al_2O_3-SiO_2. American Journal of Science, 294, 593–620.

Jenkins, D.M., and Hawthorne, F.C. (1995) Synthesis and Rietveld refinement of amphibole along the join $Ca_2Mg_5Si_8O_{22}F_2$-$NaCa_2Mg_4Ga_3Si_6O_{22}F_2$. Canadian Mineralogist, 33, 13–24.

Kunath-Fandrei, G., Bastow, T.J., Jaeger, C., and Smith, M.E. (1995) Quadrupole and chemical shift interactions of ^{27}Al in aluminium molybdate from satellite transition magic angle spinning NMR. Chemical Physics Letters, 234, 431–436.

Lippmaa, E., Samoson, A., and Mägi, M. (1986) High-resolution ^{27}Al NMR of aluminosilicates. Journal of the American Chemical Society, 108, 1730–1735.

Lowenstein, W. (1954) The distribution of aluminum in the tetrahedra of silicates and aluminates. American Mineralogist, 39, 92–96.

Makino, K., and Tomita, K. (1989) Cation distribution in the octahedral sites of hornblendes. American Mineralogist, 74, 1097–1105.

Mägi, M., Lippmaa, E., Samoson, A., Engelhardt, G., and Grimmer, A.-R. (1984) Solid-state high-resolution silicon-29 chemical shifts in silicates. Journal of Physical Chemistry, 88, 1518–1522.

Newton, R.C., Charlu, T.V., and Kleppa, O.J. (1977) Thermochemistry of high pressure garnets and clinopyroxenes in the system CaO-MgO-Al_2O_3-SiO_2. Geochimica et Cosmochimica Acta, 41, 369–377.

Oberti, R., Ungaretti, L., Cannillo, E., Hawthorne, F.C., and Memmi, I. (1995a) Temperature-dependent Al order-disorder in the tetrahedral double-chains of *C*2/*m* amphiboles. European Journal of Mineralogy, 7, 1049–1063.

Oberti, R., Hawthorne, F.C., Ungaretti, L., and Cannillo, E. (1995b) $^{[6]}$Al disorder in amphiboles from mantle peridotites. Canadian Mineralogist, 33, 867–878.

Papike, J.J., Ross, M., and Clark, J.R. (1969) Crystal-chemical characterization of clinoamphiboles based on five new structure refinements. Mineralogical Society of America, Special Paper, 2, 117–136.

Pouchou, J.L., and Pichoir, F. (1985) ''PAP'' (phi-rho-Z) procedure for improved quantitative microanalysis. In J.T. Armstrong, Ed., Microbeam Analysis, p. 104–106. San Francisco Press, San Francisco.

Raudsepp, M., Turnock, A.C., Hawthorne, F.C., Sherriff, B.L., and Hartman, J.S. (1987) Characterization of synthetic pargasitic amphiboles ($NaCa_2Mg_4M^{3+}Si_6Al_2O_{22}(OH,F)_2$; M^{3+} = Al, Cr, Ga, Sc, In) by infrared spectroscopy, Rietveld structure refinement, and ^{27}Al, ^{29}Si, and ^{19}F MAS NMR spectroscopy. American Mineralogist, 72, 580–593.

Raudsepp, M., Hawthorne, F.C., and Turnock, A.C. (1990) Evaluation of the Rietveld method for the characterization of fine-grained products of mineral synthesis: The diopside-hedenbergite join. Canadian Mineralogist, 28, 93–109.

Sherriff, B.L., and Fleet, M.E. (1990) Local ordering in gallium- and germanium-substituted glasses investigated by MAS NMR. Journal of Geophysical Research, 95, B10, 15727–15732.

Sherriff, B.L., Grundy, H.D., and Hartman, J.S. (1991) The relationship between ^{29}Si MAS NMR chemical shift and silicate mineral structure. European Journal of Mineralogy, 3, 751–768.

Skinner, B.J., and Boyd, F.R. (1964) Aluminous enstatites. Carnegie Institution of Washington Year Book, 63, 163–165.

Smelik, E.A., Jenkins, D.M., and Navrotsky, A. (1994) A calorimetric study of synthetic amphiboles along the tremolite-Tschermakite join and the heats of formation of magnesiohornblende and Tschermakite. American Mineralogist, 79, 1110–1122.

Smith, K.A., Kirkpatrick, R.J., Oldfield, E., and Henderson, D.M. (1983) High-resolution silicon-29 nuclear magnetic resonance spectroscopic study of rock-forming silicates. American Mineralogist, 68, 1206–1215.

Smith, M.E. (1993) Application of ^{27}Al NMR Techniques to Structure Determination in Solids. Applied Magnetic Resonance, 4, 1–64.

Stebbins, J.F., Sen, S., and Farnan, I. (1995): Silicate species exchange, viscosity, and crystallization in a low-silica melt: In situ high-temperature MAS NMR spectroscopy. American Mineralogist, 80, 861–864.

Stephenson, D. (1993) Amphiboles from Dalradian metasedimentary rocks of NE Scotland: Environmental inferences and distinction from amphiboles of meta-igneous amphibolites. Mineralogy and Petrology, 49, 45–62.

Strens, R.G.J. (1974) The common chain, ribbon, and ring silicates. In V.C. Farmer, Ed., The infrared spectra of minerals, p. 305–330. Mineralogical Society, London.

Warren, B.E. (1930) The crystal structure and chemical composition of the monoclinic amphiboles. Zeitschrift für Kristallographie, 72, 493–517.

Welch, M.D., Kolodziejski, W., and Klinowski, J. (1994) A multinuclear NMR study of synthetic pargasite. American Mineralogist, 79, 261–268.

Xu, Z. and Sherriff, B.L. (1993) ^{27}Al Double Rotation NMR Study of Al_2SiO_5 Polymorph minerals. Applied Magnetic Resonance, 4, 203–211.

Young, R.A. (1993) Introduction to the Rietveld method. In R.A. Young, Ed., The Rietveld method, p. 1–38. Oxford University Press, Oxford, U.K.

Manuscript received December 28, 1995
Manuscript accepted December 11, 1996